IEEE Access
Multidisciplinary | Rapid Review | Open Access Journal

Received May 9, 2020, accepted May 20, 2020, date of publication May 25, 2020, date of current version June 9, 2020.

Digital Object Identifier 10.1109/ACCESS.2020.2997252

Millimeter Wave Based Real-Time Sag Measurement and Monitoring System of Overhead Transmission Lines in a Smart Grid

AYMAN UDDIN MAHIN[1], MD. FARHAD HOSSAIN[1], (Member, IEEE), SHAMA NAZ ISLAM[2], KUMUDU S. MUNASINGHE[3], (Member, IEEE), AND ABBAS JAMALIPOUR[4], (Fellow, IEEE)

[1]Department of Electrical and Electronic Engineering, Bangladesh University of Engineering and Technology, Dhaka 1205, Bangladesh
[2]School of Engineering, Deakin University, Geelong, VIC 3216, Australia
[3]Faculty of Science and Technology, University of Canberra, Canberra, ACT 2617, Australia
[4]School of Electrical and Information Engineering, The University of Sydney, Sydney, NSW 2006, Australia

Corresponding author: Ayman Uddin Mahin (aumahin125@gmail.com)

ABSTRACT Overhead transmission line sag is a crucial parameter that needs to be measured for safe and efficient power transmission. Due to this reason, real time measurement of transmission line sag is necessary in a smart power grid. The ability of smart grid to facilitate real-time monitoring of different power system parameters allows sag measurement and monitoring of overhead transmission lines to be integrated with smart grid system. In this paper, two sag measurement methods based on millimeter wave (mmWave) signals are proposed. The performance of the proposed methods is analyzed and compared for practical 132 kV, 230 kV and 400 kV overhead power transmission lines. The first method uses single transceiver, whereas, the second method uses multiple transceivers for measuring sag. Simulation results demonstrate that the second method shows significantly better accuracy than the first method. The performance of the communication network for establishing sag related information exchange among the devices in the proposed methods is also evaluated in this paper. Moreover, trade-offs between latency and sensitivity with bandwidth, and latency and percentage average error with number of samples are also rigorously investigated.

INDEX TERMS Sag, mmWave, received power, percentage average error, shadow fading, number of samples, bandwidth, latency.

I. INTRODUCTION

Smart grid a self-monitoring advanced grid that integrates information and communication technologies to improve decision making, as well as enables efficient operation of the power system network. Moreover, it offers reliability, flexibility- through intelligent load management, automated maintenance, coordinated operation, and so on [1], [2]. Furthermore, energy flow pattern in a smart grid is more flexible compared to a traditional grid. The Energy subsystem of a smart grid can be classified into three categories: power generation [3]–[8], transmission grid [9], [10] and distribution grid [11]. Smart grid enables innovative features like advanced monitoring, control, optimization and machine learning to be included to ensure efficient transmission of power from generators to the end users. Communication technologies of a smart grid can be wireless [12]–[22] and wired [23]–[25]. The optimal operation of a smart grid system requires accurate monitoring of power system parameters. One important parameter for safe and effective operation of power system is transmission line sag, measured by the difference in height between the points of support for the transmission line and the lowest point on the conductor [26].

The placement of a transmission between two line supports can create tension on the transmission tower. If this tension crosses its limit, it can cause damage to the tower. To reduce the tension, a sag is intentionally provided in transmission line [27]. However, the sag of a line is not constant over

The associate editor coordinating the review of this manuscript and approving it for publication was Derek Abbott.

the time. In a power system, when power flows through an overhead transmission line, it heats up the line. As a result, the conductor gets extended, which increases the transmission line sag. Temporal variation of weather parameters also play role in change of sag of transmission line [28], [29]. Real-time monitoring of this variation in transmission line sag is crucial for efficient, safe and uninterrupted power transfer [30]–[32]. For instance, several studies found that the nature of rating of a transmission line is dynamic, so that capacity utilization gain can be increased between 10-30% by monitoring sag and other parameters [29], [30], [33]. Moreover, it is important to ensure a minimum ground clearance for stable and secure grid operation [34]. Increased transmission line sag can increase the chances of faults and in effect, damage the power system infrastructures. These facts necessitate real-time monitoring of the overhead high voltage transmission line sag.

On the other hand, Wireless technology is considered as the major contender for smart grid communications [1], [35]. In this essence, millimeter wave (mmWave) based wireless communication has emerged as an appropriate promising technology for real-time, fast, reliable and accurate monitoring of smart grid [36]. mmWave is the band of frequencies lies in between 30 GHz to 300 GHz. This frequencies can be used for real-time monitoring of different parameters of the system, as it offers availability and bandwidth. Moreover, size of antenna and associated network devices can be greatly reduced by incorporating mmWave in smart grid [37].

In our previous works [38], [39] on mmWave based overhead transmission line sag measurement, preliminary results have been shown on sag calculation accuracy where the impact of distance and shadowing is considered. In this paper, we present a detailed analysis of the mmWave based sag measurement methods for practical systems, under different physical system settings for three phase transmission lines. Moreover, network parameters including latency and sensitivity associated with the proposed methods are also studied rigorously in this paper. The key contributions of this paper are summarized as follows:

- Two sag measurement methods based on millimeter wave based transmission are proposed. The first method uses a transmitter and a transceiver and the second method uses an angle of arrival (AoA) sensor in addition to the transmitter and the transceiver for measuring sag of an overhead transmission line.
- Analytical models for calculating transmission line sag are developed for the proposed methods. These models incorporate the channel, device and physical system as well as communication network parameters.
- Performance of the proposed methods is evaluated and compared for practical 132 kV, 230 kV and 400 kV overhead power transmission lines in Bangladesh. In addition to the impact of channel, device and physical system parameters on sag measurement performance, the performance of the communication network in terms of latency and power consumption is also thoroughly investigated.
- The proposed mmWave methods are compared with the existing methods of measuring overhead transmission line sag.

The remainder of the paper is organized as follows. Section II describes the mmWave based sag measurement methods. Section III focuses on the performance evaluation of the methods under different system settings. Section IV demonstrates the performance of the methods from communication network perspectives, followed by a summary of the paper reflected in Section V.

II. mmWAVE BASED SAG MEASUREMENT METHODS

We propose two methods for mmWave based sag measurement. The first method does not require an AoA sensor, whereas the second one utilizes AoA measurement.

A. METHOD 1: NO AOA SENSOR

In this method, a mmWave transmitter is placed at mid-point of transmission line and a transceiver is installed on the top ground wire or the shield in such way that is equidistant from the line support. The transmitter sends a signal using mmWave frequency and the transceiver receives the signal. The received power of the mmWave signal has a direct correlation between the transmitter and the transceiver, and this distance is a function of sag. Based on the sag related information, that is received power at the transceiver, the control center in smart grid computes transmission line sag. For complete sag information, this system needs to be installed at every span of transmission lines. A schematic view of information flow in the system is shown in Fig. 1.

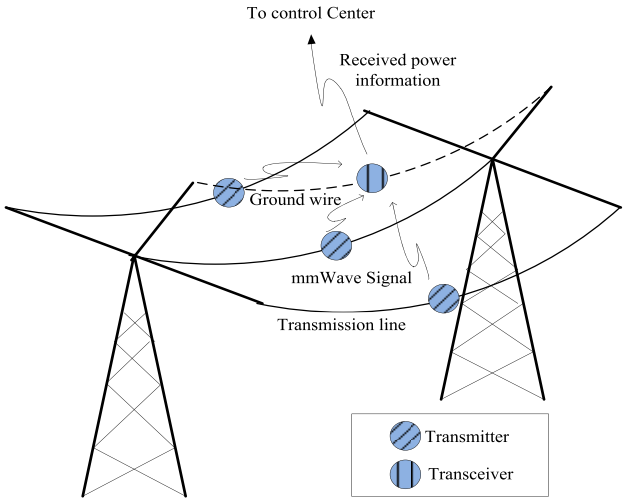

FIGURE 1. Schematic view of Method 1.

Fig. 2 (a) represents the sag measurement setup. Here, l is the span length between two adjacent towers and s is the sag of the transmission line. In Fig. 2 (b), R represents the distance between the transmitter and the transceiver. The horizontal distance between the ground wire and the transmission

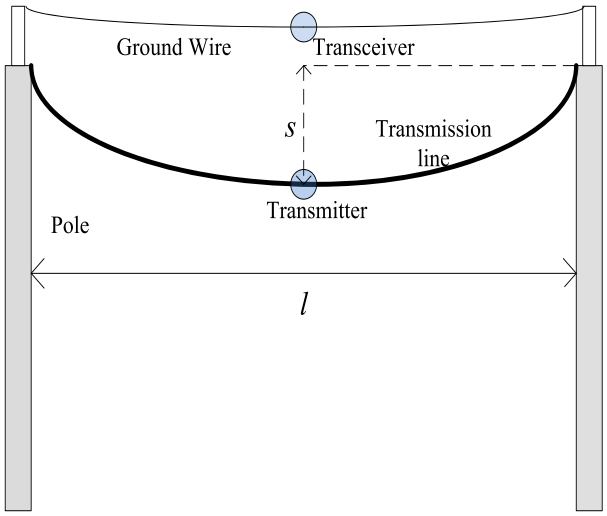

(a) Front view

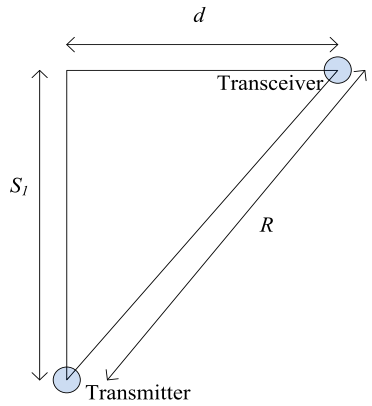

(b) Side view with related distances for sag measurement

FIGURE 2. Sag measurement setup for Method 1: No AoA sensor.

line is d. The vertical distance between the mid-point level of ground wire and the transmitter is $S_1 = \sqrt{R^2 - d^2}$.

Here, the distance S_1 can be expressed in the following manner:

$$S_1 = (d_1 + l_I + s) - S_2 \tag{1}$$

where, d_1 represents the vertical distance between the tip of ground wire support and the tip of line support, l_I denotes the length of insulator and S_2 is the sag of the ground wire. Using this method, sag for all the three lines (phase 1, phase 2 and phase 3) can be calculated. However, in that case, three transmitters are needed to be placed on the lines.

Applying Pythagorean Theorem, (2) can be extracted from Fig. 2 (b).

$$R^2 = S_1^2 + d^2 \tag{2}$$

After some algebraic manipulations in (2), sag measurement equation can be obtained as:

$$s = \sqrt{R^2 - d^2} - (l_I + d_1 - S_2) \tag{3}$$

The transmitter and the transceiver has a pure line of sight (LoS) path in between. This path loss is calculated using 5GCM path loss model designed for urban micro scenario. Equation (4) shows the path loss equation defined in the 5GCM model, where d_{3D} is the distance between transmitter and transceiver, f_c is the carrier frequency f of the transmitted signal and X_σ is zero mean Gaussian distributed random variable with standard deviation σ [40].

$$\text{PL} = 32.4 + 21\log(d_{3D}) + 20\log(f_c) + X_\sigma \tag{4}$$

After determining R based on received power or path loss from (4) and equating R with d_{3D}, transmission line sag can be determined using (3). This equation clearly indicates that this method is independent of span length, so the method is applicable for longer transmission lines as well.

B. METHOD 2: WITH AOA SENSOR

In this method, a transceiver along with an AoA sensor is placed on the transmission line at the end of the span and a transmitter can be installed at any point on the conductor. The mmWave signal is sent to the transceiver at regular intervals to identify any changes occurring in real-time.

The received power and the AoA of the signal changes with sag of the line. The AoA sensor determines the AoA of the incoming mmWave signal. The transceiver sends received power and AoA information to the control center of the smart grid. Depending on the received power level and AoA, location of the transmitter is determined to calculate the sag. The shape of a transmission line placed in between two transmission towers can be approximated as a parabola, assuming smaller sag compared to the span length of the line [27]. This approximation is considered for sag calculation in this method.

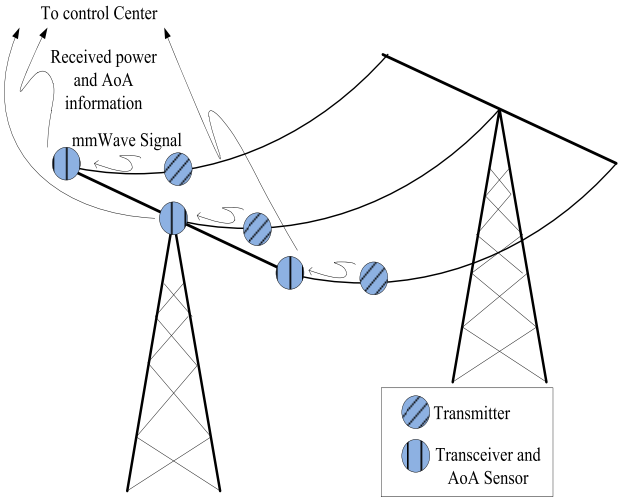

FIGURE 3. Schematic view of Method 2.

Fig. 3 shows the schematic view of the method and Fig. 4 represents the sag measurement setup. Here, l is the distance between two line supports and s represents the sag. The vertical distance between the transmitter and the

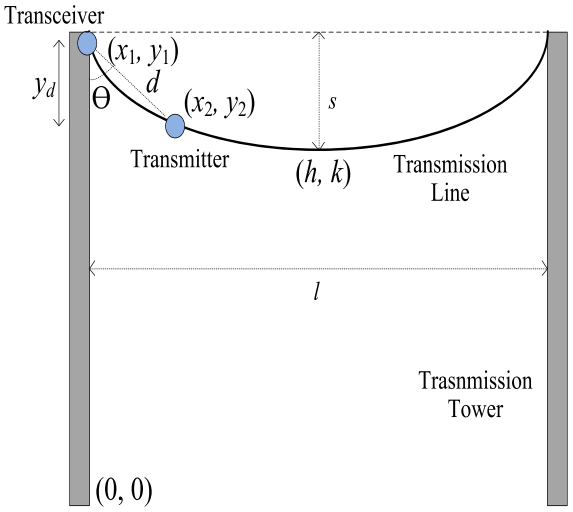

FIGURE 4. Sag measurement setup.

transceiver is y_d, (x_1, y_1) is the location of the transceiver and (x_2, y_2) is the location of the transmitter. General equation of a parabola can be written as (5). Where, (h, k) is the vertex and a represents the coefficient.

$$y = a(x - h)^2 + k \tag{5}$$

Assuming mid-point of the transmission line, $h = l/2$. Thus (5) becomes:

$$y = a(x - l/2)^2 + k \tag{6}$$

For the transceiver and the transmitter locations, (7) and (8) are obtained from (6).

$$y_1 = a(x_1 - l/2)^2 + k \tag{7}$$

$$y_2 = a(x_2 - l/2)^2 + k \tag{8}$$

From (7),

$$k = y_1 - a(x_1 - l/2)^2 \tag{9}$$

Substituting (9) into (8), the coefficient is expressed as:

$$a = \frac{y_2 - y_2}{(x_2 - l/2)^2 - (x_1 - l/2)^2} \tag{10}$$

Now, from (9) and (10), (11) of sag can be determined, where, $s = (y_1 - k)$.

$$s = (x_1 - 0.5l)^2 \frac{(y_2 - y_1)}{\{(x_2 - 0.5l)^2 - (x_1 - 0.5l)^2\}} \tag{11}$$

In this method, the transceiver position (x_1, y_1) is fixed and known but the transmitter position (x_2, y_2) varies with sag. We use 5GCM path loss model according to (4) to calculate d based on the received power. Note that the variation in d will be smaller with small value of sag. However, for larger sag, the transmitter's position will change. Moreover, physical measurement of the sag with good accuracy may not always be possible. Thus, measuring distance from the path loss model can serve as an accurate and automated way for sag calculation.

Once d is determined, location (x_2, y_2) of the transmitter is determined using:

$$x_2 = d\cos\theta \tag{12}$$

$$y_2 = y_1 - d\sin\theta \tag{13}$$

After the transmitter position is determined, sag is calculated from (11). As this method does not have any dependency on ground wire and distance between transmitter and transceiver is same for all the three phases of transmission line, impact of different parameters will be same for the lines. On the other hand, impact of different parameters is different for the lines in Method 1.

III. PERFORMANCE ANALYSIS: IMPACT OF SYSTEM PARAMETERS

In this section, we investigate how channel parameters like shadow fading, device parameters like number of samples influence the performance of the proposed methods. We also evaluate the impact of physical system parameters like span length, AoA and horizontal distance on sag measurement accuracy. To study the impact of these parameters, three practical transmission tower geometries are used for 132 kV, 230 kV and 400 kV transmission lines in Bangladesh are considered. Fig. 5 shows practical double circuit suspension transmission towers for 132 kV, 230 kV and 400 kV lines along with dimensions. For 132 kV double circuit transmission lines, single ground wire is used. On the other hand, two ground wires are used for 230 kV and 400 kV transmission lines. Typical span lengths for 132 kV, 230 kV and 400 kV transmission lines are 330 m, 380 m and 375 m, respectively.

A. IMPACT OF SHADOW FADING

Shadow fading level is an important parameter that influences transmission line sag calculation. In any kind of wireless environment, path loss is subject to shadowing. Thus, calculation error increases with shadowing. In this analysis, we considered a shadow fading of 3.76 dB according to the path loss model in [40]. Then we also investigated how different levels of shadowing influence the sag calculation error. Fig. 6 shows the impact of shadow fading on sag calculation for phase 1 transmission lines in 132 kV, 230 kV and 400 kV systems when Method 1 is used. Similar analysis can be carried out for phase 2 and phase 3 lines as well. Fig. 7 shows the impact of shadow fading when Method 2 is used. For calculating one value of a sag, 20 samples of received power are collected, and frequency and AoA error are considered 30 GHz and 0 degree, respectively. It clear that for higher value of standard deviation of shadowing, the calculated value of sag differs more from the actual value in Method 1. On the other hand, Impact of shadow fading is significantly lower for all the lines in Method 2. For instance, percentage average error is 12.4 % for 132 kV phase 1 line in Method 1, while, the error is 0.33 % for the same line in Method 2. For method 2, we can consider that the transmitter is chosen to be placed closer to the transceiver, and so the impact of shadow fading becomes less, as observed in the numerical results.

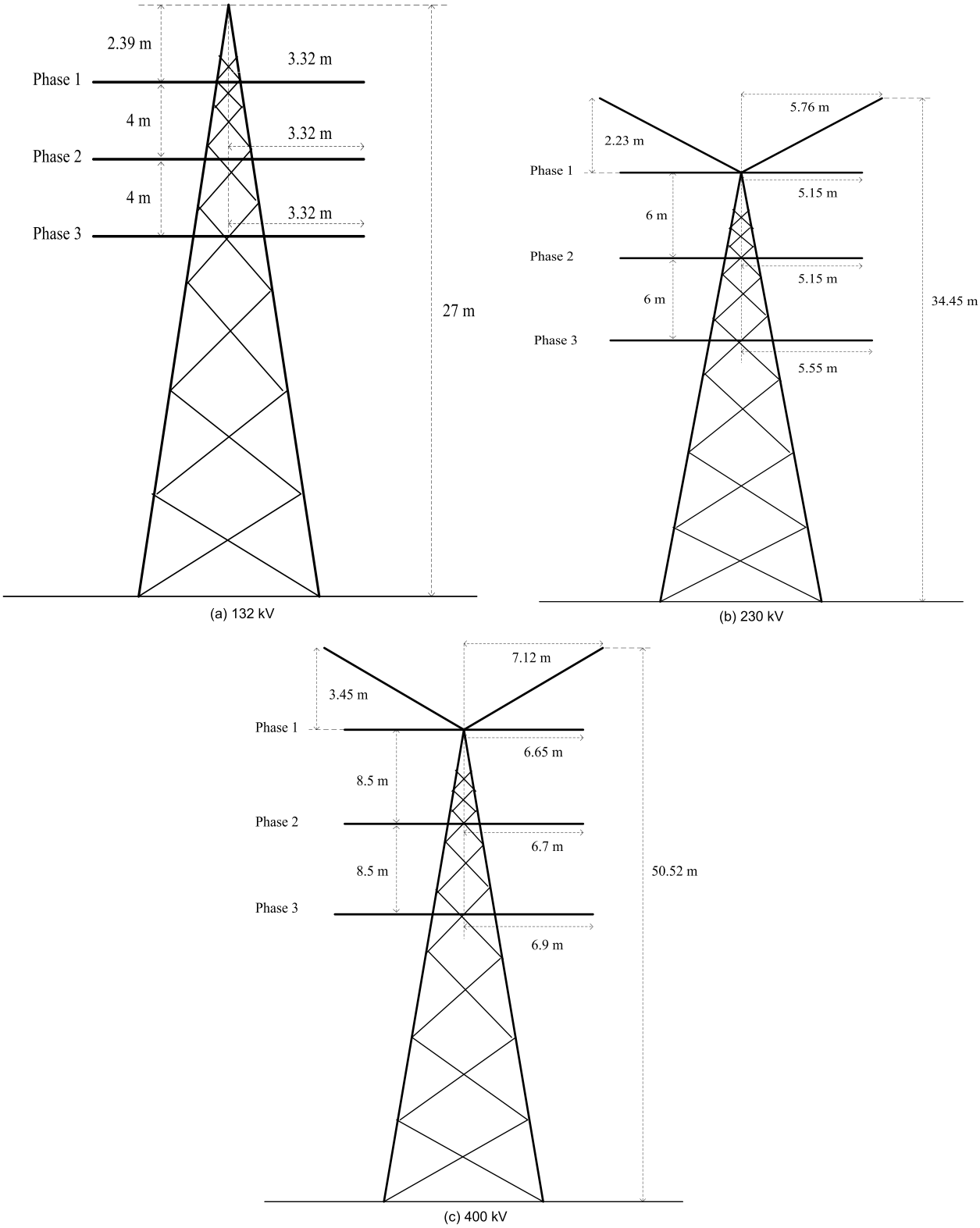

FIGURE 5. Practical high voltage power transmission tower.

B. IMPACT OF NUMBER OF SAMPLES

Number of samples (n) indicates number of measurements collected in a given time frame for calculating single value of sag. For Method 1, sag related information is received power level. On the other hand, received power level and AoA are the sag related information in Method 2. With more

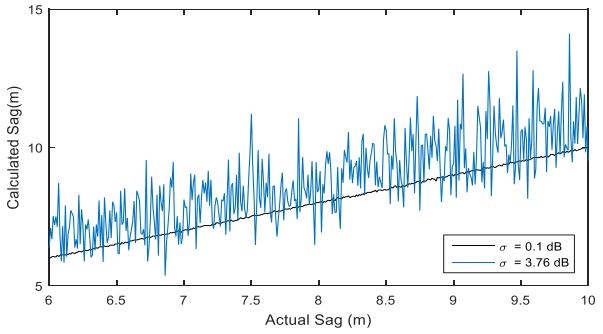

(a) 132 kV

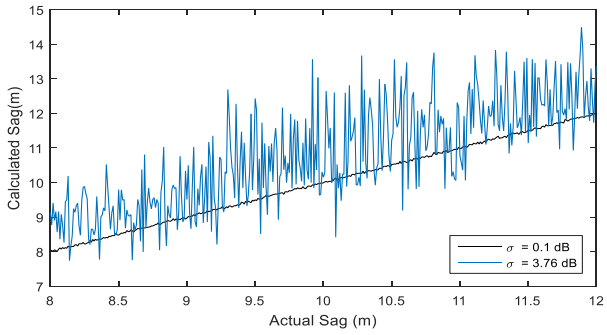

(b) 230 kV

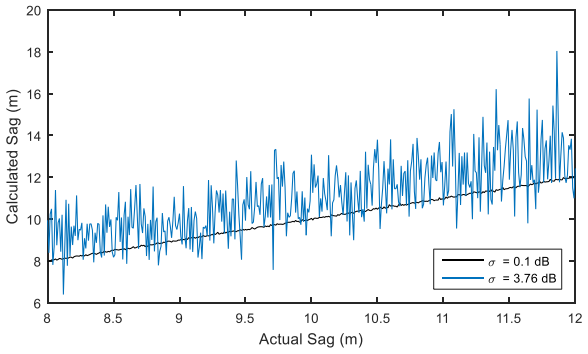

(c) 400 kV

FIGURE 6. Impact of shadow fading on sag calculation for phase 1 of different transmission networks using Method 1.

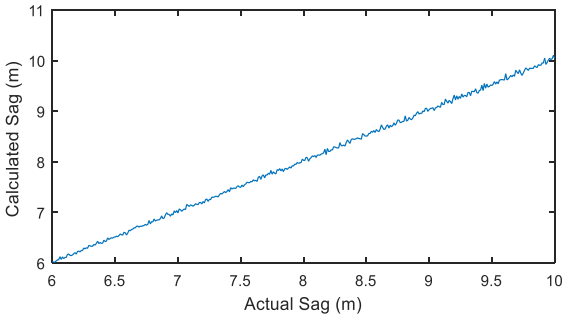

(a) 132 kV

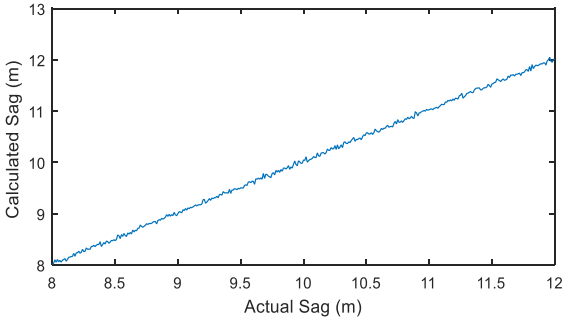

(b) 230 kV

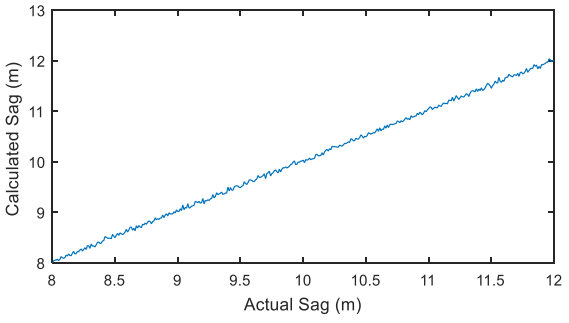

(c) 400 kV

FIGURE 7. Impact of shadow fading on sag calculation for all phases of different transmission networks using Method 2.

number of samples, sag calculation accuracy increases. At the same time, it requires increased charge storing capacity of the devices. Fig. 8 and Fig. 9 shows the impact of number of samples on the accuracy of the calculated value in Method 1 and Method 2, respectively for 230 kV transmission lines. Similar results can be obtained for the other lines. It is visible that even with the smaller number of samples, more accurate sag calculation is possible in Method 2, compared to Method 1. For example, percentage average error is 7.5 % for 230 kV top line in Method 1 for 100 samples. On the other hand, error is 0.28 % for the same number samples and same line in Method 2.

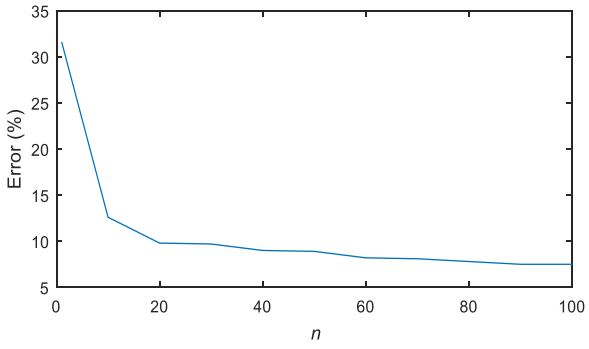

FIGURE 8. Impact of number of samples on phase 1 of 230 kV transmission line in Method 1.

C. IMPACT OF HORIZONTAL DISTANCE

In this section, we evaluate the impact of horizontal distance between transmitter and transceiver d. For Method 1, this distance can vary for the three phases of the transmission line, depending on the support. Fig. 10 shows the impact of d on the calculated sag for phase 1 of 230 kV transmission

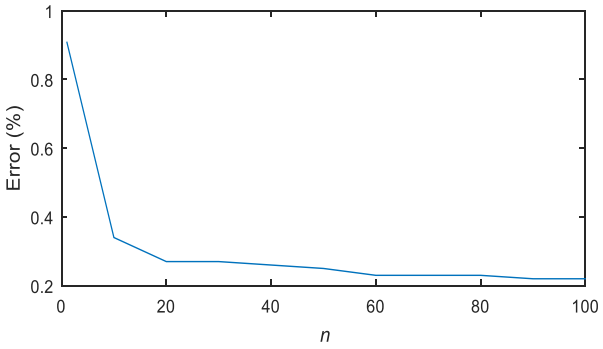

FIGURE 9. Impact of n on 230 kV transmission lines in Method 2.

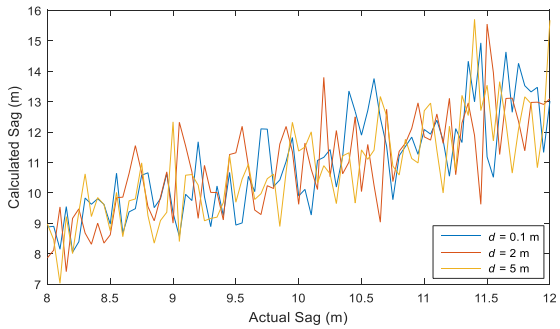

FIGURE 10. Impact of d on phase 1 of 230 kV transmission line in Method 1.

line in Method 1. Three distance values are considered, $d = 0.1$ m, $d = 2$ m and $d = 5$ m. With the increase in d, error increases as the difference between the calculated sag and the actual value increases. To reduce error, the transceiver should be placed on the ground wire close to the transmission line in Method 1. Similarly, when the horizontal distance between the transmitter and the transceiver x_2 increases, error in calculated sag in Method 2 increases as shown in Fig. 11.

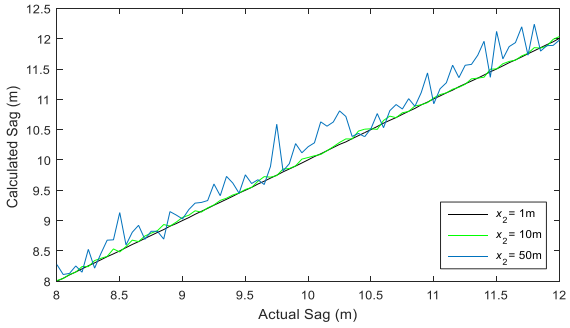

FIGURE 11. Impact of x_2 on 230 kV transmission lines in Method 2.

D. IMPACT OF ANGLE OF ARRIVAL (AoA)

Error in measurement of AoA θ_e is an important factor for sag calculation accuracy in Method 2, whereas, Method 1 is free from this kind of error. When sag is small, small error in AoA measurement can amplify the error in the calculated sag. However, with higher value of sag, error decreases. Impact of AoA on the average error for $\sigma = 0$ dB and 20 samples

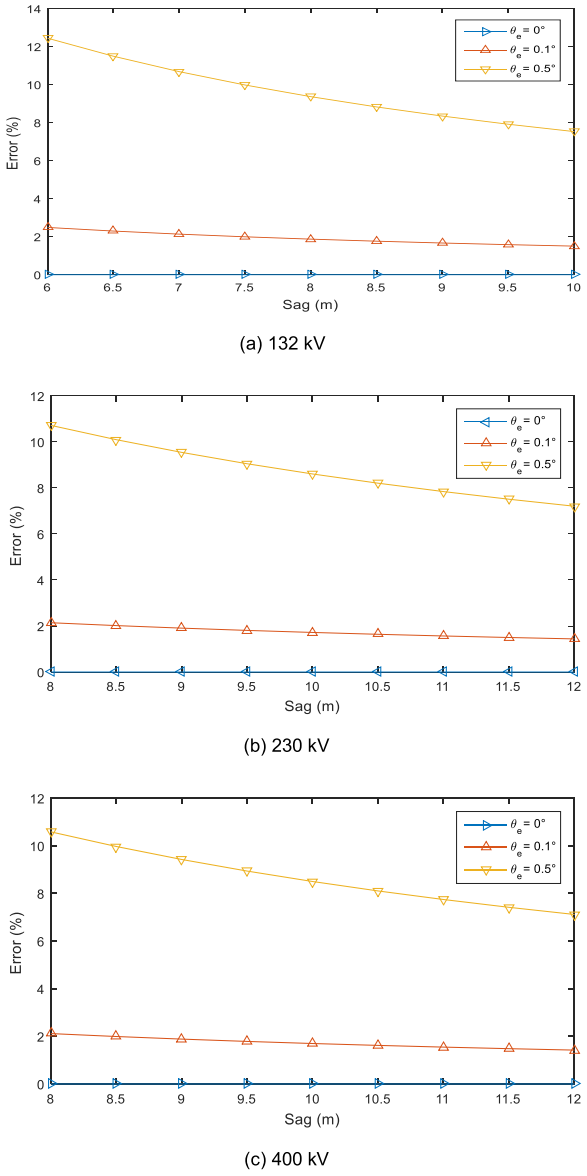

FIGURE 12. Impact of θ_e on (a) 132 kV (b) 230 kV and (c) 400 kV lines in Method 2.

is shown in Fig. 12. It is shown that the percentage error in calculated sag decreases with increase in sag and the error is significantly high for high AoA measurement error. For instance, percentage average error is 1.92 % for 132 kV line at AoA error of 0.1 degree, while the error is 9.62 % for the same line at 0.5 degree AoA error. However, error in AoA can be considered close to 0 degree at moderate SNR when multiple antenna elements are considered [41].

E. IMPACT OF SPAN LENGTH

Span length can be different for different sections of transmission lines. Span length of a section can have impact on the accuracy of the calculated sag in Method 2, whereas, Method 1 is free from the impact of span length. For long span length, distance between the transmitter and the transceiver

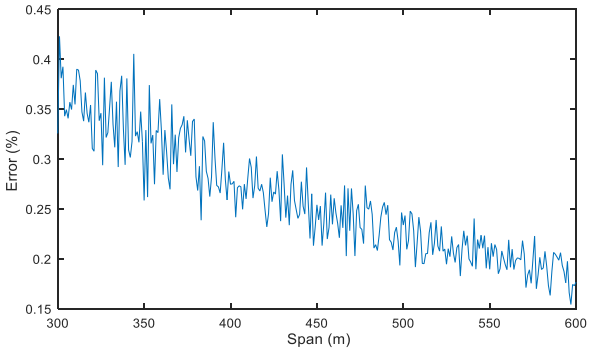

FIGURE 13. Impact of span length on error in calculated sag in Method 2.

increases slowly with the sag of the line. On the other hand, the distance between the devices increases at relatively higher rate for shorter span length. Due to this reason, percentage of error in calculated sag is relatively lower for transmission line with longer span length. Fig. 13 demonstrates the relation between span length and average sag calculation error for a transmission line considering 20 samples of received power, frequency of 30 GHz and shadow fading standard deviation of 3.76 dB. The transmitter is considered to be placed at 10 m away horizontally from the transceiver.

IV. PERFORMANCE ANALYSIS: NETWORKING PERSPECTIVE

In this section, we evaluate the communication network performance which is critical for sag related information transmission and sag calculation.

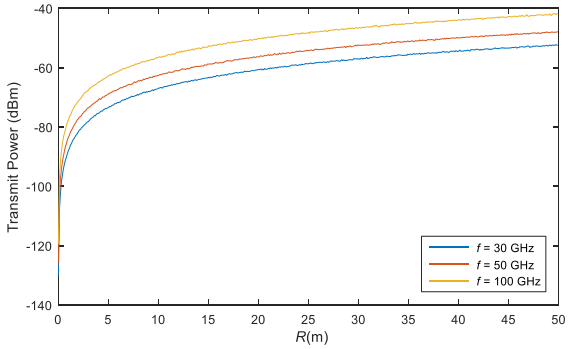

FIGURE 14. Minimum transmit power for different frequencies.

A. IMPACT OF FREQUENCY ON TRANSMIT POWER

For extracting the transmitted mmWave signal at the transceiver, a minimum transmit power is required for the transmitter. The minimum transmit power is dependent on the maximum distance that occurs during the variation of sag, receiver sensitivity and frequency. The maximum distance between the transmitter and the transceiver is different for 132kV, 230 kV and 400 kV lines. Fig. 14 shows minimum transmit power requirement for transmitter for variation of distance R between the transmitter and the transceiver for different frequencies f. For this simulation, the transceiver sensitivity is considered -150 dBm. For higher R and f, minimum transmit power requirement is higher.

B. COMMUNICATION FRAMES

For transferring sag related information to the control center, message frames are produced. For Method 1, sag related information is received power level, while, received power level and AoA are the sag related information for Method 2. Received power P_r by the transceiver can be expressed as (14), where $d_i, i = 1, 2 \ldots, 7$ represents the digit of P_r. Similarly, AoA can be expressed by (15), where $A_i, i = 1, 2 \ldots, 7$ represents the digit of AoA. A 7 digit number and a 6 digit number can be represented by 24 bits and 20 bits, respectively.

$$P_r = -d_1 d_2 d_3 \cdot d_4 d_5 d_6 d_7 \text{ dBm} \quad (14)$$

$$\text{Angle of arrival} = -A_1 A_2 \cdot A_3 A_4 A_5 A_6^{\circ} \quad (15)$$

Four digits after decimal point is taken for achieving resolution of 0.1 cm. Method 1 includes the digits of received power in the frame. On the other hand, Method 2 contains the digits of received power and AoA. A device identification (ID) number for the transceiver is also added to the frame. The control center has the information for the corresponding devices. Number of bits for device ID k is dependent on the number of transceiver under a control center. After extracting the transmitted information from the frame, sag is calculated using one of the two methods. Fig. 15 shows the frames for conveying sag related information in the two methods.

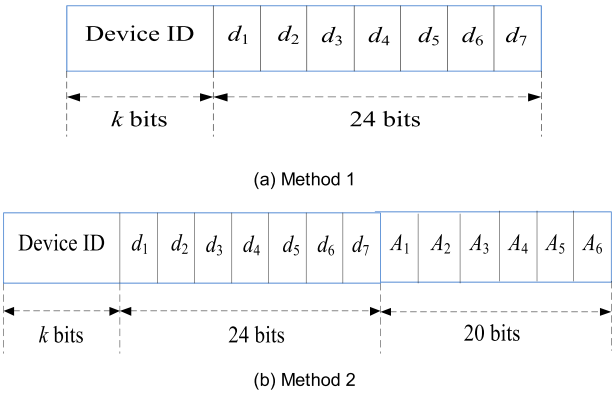

FIGURE 15. Message frame for communicating sag related information.

After the communication frames are constructed at the transceiver, it sends the information using mmWave frequencies to the nearby small-cell base station, which supports short range communication. The small-cell base station can then use the core network to forward the message to the control center through the central server. The transmission technique is similar to the one adopted by 5G technologies. Given that this paper mainly focusses on sag calculation methods, further details are not discussed on data transmission as it is not within the scope of this paper.

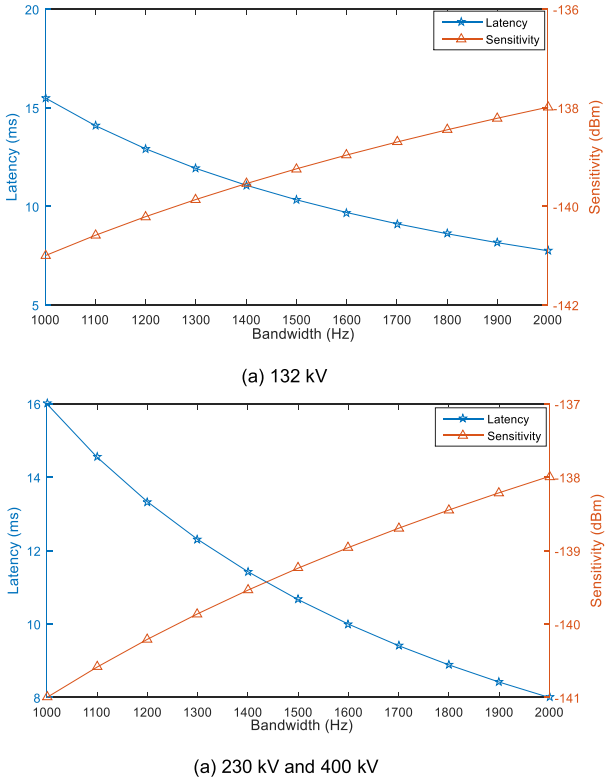

FIGURE 16. Latency for a message frame and receiver sensitivity with bandwidth in Method 1.

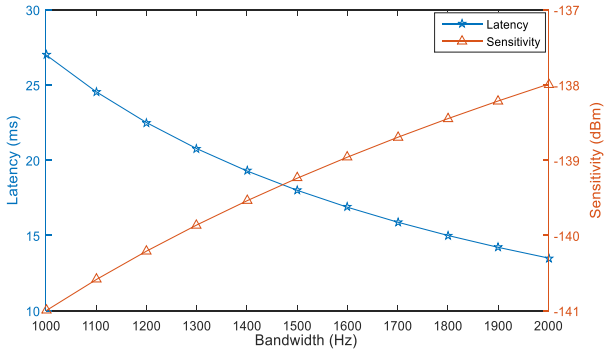

FIGURE 17. Latency for a message frame and receiver sensitivity with bandwidth in Method 2.

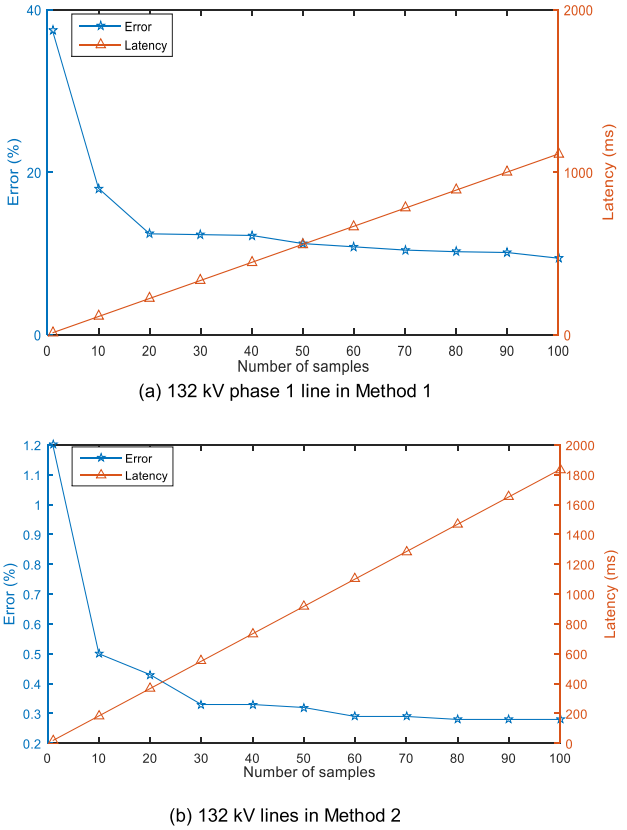

FIGURE 18. Trade-off between sag calculation error with the number of samples.

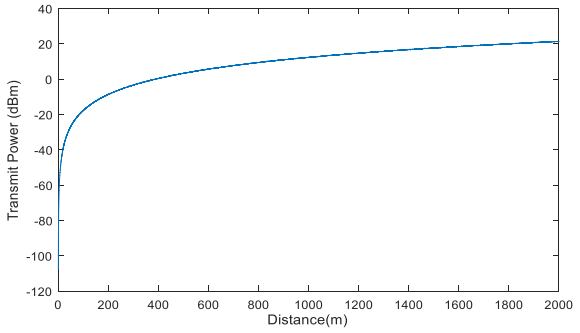

FIGURE 19. Variation of transceiver transmit power with distance for 132 kV line in Method 1.

C. LATENCY AND SENSITIVITY

In this subsection, we evaluate the latency and sensitivity of the sag measurement methods. For transmitting sag related information to the control center, a bandwidth B is allocated to the transceiver. Sensitivity of the receiver is dependent on the bandwidth of the signal. Equation (16) shows the relation of receiver sensitivity with bandwidth [42]. Where, S is the sensitivity of the receiver, NF is noise figure and SNR_{min} is minimum SNR requirement. Sensitivity of a receiver decreases with increase in bandwidth. On the other hand, according to Shannon's capacity shown in (17), bit rate C is proportional to the bandwidth [43]. The latency is based on the frame duration. The transmission time is assumed to be negligible compared to the frame duration. The latency is calculated using (18), where, L is latency, T_b is bit duration, N_b is number of bits in a frame and n is number of samples.

$$S = -174\text{dBm} + 10\log(B) + \text{NF} + \text{SNR}_{\text{min}} \quad (16)$$

$$C = B\log_2(1 + \text{SNR}) \quad (17)$$

$$L = T_b \times N_b \times n \quad (18)$$

Fig. 16 and Fig. 17 show the dependency of sensitivity and latency for a message frame in Method 1 and 2, respectively on the bandwidth. In this case, 3 dB SNR and 0 noise figure are considered. Bandwidth of the transmitted signal from the transceiver is varied from 1 kHz to 2 kHz and impact on the receiver sensitivity at the base station and latency per

TABLE 1. Comparison Between mmWave Based Methods.

Parameter		Average error (%)					
		Method 1			Method 2		
		132 kV (Top line)	230 kV (Top line)	400 kV (Top line)	132 kV (All lines)	230 kV (All lines)	400 kV (All lines)
σ (dB) (n =20) ($\theta_e = 0^\circ$)	0.1	0.23	0.16	0.23	0.0064	0.0054	0.0052
	1	2.3	1.81	2.18	0.0598	0.0543	0.0561
	3.76	12.4	9.45	11.64	0.3300	0.2889	0.2863
n (σ= 3.76 dB) ($\theta_e = 0^\circ$)	10	18	12.6	16.5	0.48	0.33	0.38
	20	12.4	9.8	11.64	0.43	0.27	0.32
	50	11.2	8.9	11.4	0.32	0.25	0.26
	100	9.4	7.5	9.7	0.28	0.23	0.24
θ_e (degree) (σ=0 dB) (n =20)	0	0	0	0	0	0	0
	0.5	0	0	0	1.92	1.74	1.72
	1	0	0	0	9.62	8.75	8.64
Optimum Bandwidth (Hz)		1395	1436	1436	1471	1471	1471
Frame duration (ms)		11.11	11.14	11.14	18.35	18.35	18.35

frame is observed. 100 number of segments of transmission line are considered for simulation. For 100 segments, number of transceivers is 100 for 132 kV lines and 200 for 230 kV and 400 kV lines in Method 1. So, value of k is 7 for 132 kV lines and 8 for 230 kV and 400 kV lines in this method. In Method 2, for 100 segments, there are 600 transceivers for all types of transmission lines in this method. So, value of k is 10 for 132 kV, 230 kV and 400 kV lines in this case.

As sensitivity of the receiver decreases and latency per frame increases with bandwidth, a trade- off is required for selecting optimum bandwidth for data transmission. From Fig. 16 and Fig. 17, optimum bandwidths can be found from the trade-off between the latency and sensitivity. In Method 1, optimum bandwidths are 1395 Hz for 132 kV lines and 1436 Hz for 230 kV and 400 kV lines. Sensitivity is −139.6 dBm and latency per frame is 11.11 ms for 132 kV lines. For 230 kV and 400 kV lines, sensitivity and latency per frame are −139.4 dBm and 11.14 ms, respectively in this method. On the other hand, optimum bandwidth is 1471 Hz, for which sensitivity is −139.3 dBm and latency per frame is 18.35 ms in Method 2.

In both methods, percentage error in sag calculation decreases and latency increases with number of samples. So, trade-offs are also required in these cases. Fig. 18 (a) and 18 (b) show the change of percentage error and latency with number of samples for phase 1 of 132 kV lines in Method 1 and for all 132 kV lines in Method 2, respectively.

TABLE 2. Comparison Among Different Methods of Measuring Sag.

No.	Methods	Hardware Requirements	Advantages	Disadvantages	Remarks
1.	Proposed mmWave based Method 1	• Transmitter • Transceiver	• Simple in Operation • Doesn't need complex algorithm • Allows real time monitoring • Low latency	• High impact of shadow fading • Requirement of overhead ground wire • Alignment requirement between transmitter and transceiver	• Resolution= 0.1 cm
2.	Proposed mmWave based Method 2	• Transmitter • Transceiver with AoA sensor	• Low error • Doesn't require overhead ground wire • Low impact of shadowing on calculated sag • Allows real-time monitoring • Low latency	• High impact of AoA error • Higher number of transceivers • Higher latency compared to method 1	• Resolution= 0.1 cm
3.	DGPS based [31, 34, 44]	• Rover transceiver • Base transceiver • Digital signal processor • DC power supply	• Independent of parameters like weather condition, temperature, tension • Low cost Operation in all weather conditions	• Complex algorithm • Requires satellites • Requires number of components	• Accuracy of approximately 2.54 cm • Error < 5%
4.	GPS based [45]	• Polymer Insulator • GPS receiver • Bluetooth device	• Incorporates accuracy enhancement techniques • Allows real-time monitoring	• Complex algorithm • Requires satellites • Large in size	• Error of approximately 25 cm in sag calculation
5.	Current and flux density based [46, 47]	• Magnetic field sensor • Current transformer • Microcontroller • Signal conditioner and amplifier • Communication circuitry	• Low cost • Good accuracy	• Synchronization between MF data and EC data is required	• Error < 1% of the conductor length
6.	Temperature based [33, 48]	• Temperature sensors	• Only uses one parameter to calculate sag	• Variation of temperature in power line occurs in both axial and radial directions	• High error
7.	Tension based [27]	• Load cells	• Sag can be determined using only one parameter (tension) • Outage is required for installation	• High precision is required for determining change in tension.	• High error
8.	Laser technique [49, 50]	• Optical device	• High accuracy	• Expensive • Requires human presence • Not suitable of real-time monitoring	• Accuracy = 0.6 cm

D. TRANSCEIVER TRANSMIT POWER

For a particular frequency transmit power requirement of a transceiver depends on the sensitivity of the receiver and the distance between the transceiver and the receiver. Transmit power requirement increases with increase distance between the transceiver and the receiver. For Method 1, receiver sensitivities are −139.6 dBm for 132 kV lines and −139.4 dBm for 230 kV and 400 kV lines. On the other hand, receiver sensitivity is −139.3 dBm for all lines in Method 2. So, the optimum sensitivities are almost same for all the lines in both methods. Due to this, variation of transceiver transmit power with distance is similar for both methods. Fig. 19 Shows the variation of the transceiver transmit power with the distance between the transceiver and the receiver for 132 kV line in Method 1 at 30 GHz frequency. For calculating path loss, 5GCM path loss model for non-line-of-sight as shown in equation (19) is used [40]. Here, standard deviation of shadow fading is 6.8.

$$\mathrm{PL} = 32.4 + 30\log(d_{3D}) + 20\log(f_c) + X_\sigma \qquad (19)$$

A comparison between the mmWave based methods are shown in Table 1. It is clear that impact of shadowing is significantly lower for Method 2, compared to Method 1. In the case of number of samples, better accuracy can be achieved with lower number of samples in Method 2. On the other hand, Method 2 faces error due to AoA error. Moreover, optimum bandwidth and frame duration are also relatively higher for Method 2.

A comparison between different techniques of measuring sag is presented in Table 2. The mmWave based methods are simple in operation and provide a very high resolution of 0.1 cm. Moreover, the mmWave based methods also allow real-time monitoring with low latency. However, accuracy of the proposed methods can be affected by natural factors, for instance, wind and ice loading. The environmental factors can also cause inaccuracies in distance calculation using the path loss model. Furthermore, data loss during transmission of sag related information has potential to cause error in sag calculation.

V. CONCLUSIONS

In this paper, two mmWave based overhead transmission line sag measurement methods have been proposed and performance of the proposed methods has been analyzed for practical 132 kV, 230 kV and 400 kV transmission lines. The methods are simple in operation and does not require any complex algorithm for calculation of sag. The methods also offer a very high resolution of 0.1 cm. Impact of different system parameters, namely, number of samples, shadow fading, horizontal distance between the transmitter and the transceiver, AoA error and span length has been thoroughly investigated for practical transmission lines. The effect of shadow fading is significantly lower in the case of Method 2, compared to Method 1. Method 2 allows more accurate sag calculation even with smaller number of samples. On the other hand, Method 2 faces errors in sag calculation due to AoA measurement error, while, Method 1 is free from this type of error. Moreover, the percentage error decreases with increase in span length in Method 2. Performance of the proposed methods from communication network perspective in terms of latency, bandwidth, etc. has also been investigated in this paper. Simulation results have demonstrated that latency per frame and sensitivity of the receiver decrease with bandwidth. Due to this, a trade-off has been obtained between latency and sensitivity to optimize bandwidth for transmission of frames to the control center. In future, the proposed methods will be tested over a network of transmitters and transceivers which will coordinate the sag estimations for a number of transmission line segments.

REFERENCES

[1] R. Ma, H.-H. Chen, Y.-R. Huang, and W. Meng, "Smart grid communication: Its challenges and opportunities," *IEEE Trans. Smart Grid*, vol. 4, no. 1, pp. 36–46, Mar. 2013.

[2] X. Fang, S. Misra, G. Xue, and D. Yang, "Smart grid—The new and improved power grid: A survey," *IEEE Commun. Surveys Tuts.*, vol. 14, no. 4, pp. 944–980, 4th Quart., 2012.

[3] P. B. Andersen, B. Poulsen, M. Decker, C. Traeholt, and J. Ostergaard, "Evaluation of a generic virtual power plant framework using service oriented architecture," in *Proc. IEEE 2nd Int. Power Energy Conf.*, Johor Bahru, Malaysia, Dec. 2008, pp. 1212–1217.

[4] B. Jansen, C. Binding, O. Sundstrom, and D. Gantenbein, "Architecture and communication of an electric vehicle virtual power plant," in *Proc. 1st IEEE Int. Conf. Smart Grid Commun.*, Gaithersburg, MD, USA, Oct. 2010, pp. 149–154.

[5] P. Lombardi, M. Powalko, and K. Rudion, "Optimal operation of a virtual power plant," in *Proc. IEEE Power Energy Soc. Gen. Meeting*, Calgary, AB, Canada, Jul. 2009.

[6] A. Molderink, V. Bakker, M. G. C. Bosman, J. L. Hurink, and G. J. M. Smit, "Management and control of domestic smart grid technology," *IEEE Trans. Smart Grid*, vol. 1, no. 2, pp. 109–119, Sep. 2010.

[7] S. You, C. Traeholt, and B. Poulsen, "A market-based virtual power plant," in *Proc. Int. Conf. Clean Electr. Power*, Capri, Italy, Jun. 2009, pp. 460–465.

[8] S. You, C. Traeholt, and B. Poulsen, "Generic virtual power plants: Management of distributed energy resources under liberalized electricity market," in *Proc. 8th Int. Conf. Adv. Power Syst. Control, Operation Manage. (APSCOM)*, Hong Kong, 2009, pp. 1–6.

[9] F. Li, W. Qiao, H. Sun, H. Wan, J. Wang, Y. Xia, Z. Xu, and P. Zhang, "Smart transmission grid: Vision and framework," *IEEE Trans. Smart Grid*, vol. 1, no. 2, pp. 168–177, Sep. 2010.

[10] A. Bose, "Smart transmission grid applications and their supporting infrastructure," *IEEE Trans. Smart Grid*, vol. 1, no. 1, pp. 11–19, Jun. 2010.

[11] T. Takuno, M. Koyama, and T. Hikihara, "In-home power distribution systems by circuit switching and power packet dispatching," in *Proc. 1st IEEE Int. Conf. Smart Grid Commun.*, Gaithersburg, MD, USA, Oct. 2010, pp. 427–430.

[12] I. F. Akyildiz and X. Wang, "A survey on wireless mesh networks," *IEEE Commun. Mag.*, vol. 43, no. 9, pp. S23–S30, Sep. 2005.

[13] H. Gharavi and B. Hu, "Multigate communication network for smart grid," *Proc. IEEE*, vol. 99, no. 6, pp. 1028–1045, Jun. 2011.

[14] V. C. Gungor and F. C. Lambert, "A survey on communication networks for electric system automation," *Comput. Netw.*, vol. 50, no. 7, pp. 877–897, May 2006.

[15] K. S. Hung, W. K. Lee, V. O. K. Li, K. S. Lui, P. W. T. Pong, K. K. Y. Wong, G. H. Yang, and J. Zhong, "On wireless sensors communication for overhead transmission line monitoring in power delivery systems," in *Proc. 1st IEEE Int. Conf. Smart Grid Commun.*, Gaithersburg, MD, USA, Oct. 2010, pp. 309–314.

[16] A. Ghassemi, S. Bavarian, and L. Lampe, "Cognitive radio for smart grid communications," in *Proc. 1st IEEE Int. Conf. Smart Grid Commun.*, Gaithersburg, MD, USA, Oct. 2010, pp. 297–302.

[17] X. Ma, H. Li, and S. Djouadi, "Networked system state estimation in smart grid over cognitive radio infrastructures," in *Proc. 45th Annu. Conf. Inf. Sci. Syst.*, Baltimore, MD, USA, Mar. 2011, pp. 1–5.
[18] R. C. Qiu, Z. Chen, N. Guo, Y. Song, P. Zhang, H. Li, and L. Lai, "Towards a real-time cognitive radio network testbed: Architecture, hardware platform, and application to smart grid," in *Proc. 5th IEEE Workshop Netw. Technol. Softw. Defined Radio Netw. (SDR)*, Boston, MA, USA, Jun. 2010, pp. 1–6.
[19] R. C. Qiu, Z. Hu, Z. Chen, N. Guo, R. Ranganathan, S. Hou, and G. Zheng, "Cognitive radio network for the smart grid: Experimental system architecture, control algorithms, security, and microgrid testbed," *IEEE Trans. Smart Grid*, vol. 2, no. 4, pp. 724–740, Dec. 2011.
[20] A. A. Sreesha, S. Somal, and I.-T. Lu, "Cognitive radio based wireless sensor network architecture for smart grid utility," in *Proc. IEEE Long Island Syst., Appl. Technol. Conf.*, Farmingdale, NY, USA, May 2011, pp. 1–7.
[21] U. D. Deep, B. R. Petersen, and J. Meng, "A smart microcontroller-based iridium satellite-communication architecture for a remote renewable energy source," *IEEE Trans. Power Del.*, vol. 24, no. 4, pp. 1869–1875, Oct. 2009.
[22] P. Yi, A. Iwayemi, and C. Zhou, "Developing ZigBee deployment guideline under WiFi interference for smart grid applications," *IEEE Trans. Smart Grid*, vol. 2, no. 1, pp. 110–120, Mar. 2011.
[23] M. McGranaghan and F. Goodman, "Technical and system requirements for advanced distribution automation," in *Proc. 18th Int. Conf. Exhib. Electr. Distrib. (CIRED)*, Turin, Italy, 2005, pp. 1–5.
[24] S. Galli, "A simplified model for the indoor power line channel," in *Proc. IEEE Int. Symp. Power Line Commun. Appl.*, Dresden, Germany, Mar. 2009, pp. 13–19.
[25] S. Galli, A. Scaglione, and K. Dostert, "Broadband is power: Internet access through the power line network," *IEEE Commun. Mag.*, vol. 41, no. 5, pp. 82–83, May 2003.
[26] MENSAH-BONSU and Heydt, "Overhead transmission conductor sag: A novel measurement technique and the relation of sag to real time circuit ratings," *Electr. Power Compon. Syst.*, vol. 31, no. 1, pp. 61–69, Jan. 2003.
[27] V. K. Mehta and R. Mehta, "Mechanical design of overhead lines," in *Prince Power Systems*, 4th ed. New Delhi, India: S. Chand Company, 2006, ch. 8, pp. 186–201.
[28] W. de Villiers, J. H. Cloete, L. M. Wedepohl, and A. Burger, "Real-time sag monitoring system for high-voltage overhead transmission lines based on power-line carrier signal behavior," *IEEE Trans. Power Del.*, vol. 23, no. 1, pp. 389–395, Jan. 2008.
[29] A. Michiorri, H. M. Nguyen, S. Alessandrini, J. B. Bremnes, S. Dierer, E. Ferrero, B.-E. Nygaard, P. Pinson, N. Thomaidis, and S. Uski, "Forecasting for dynamic line rating," *Renew. Sustain. Energy Rev.*, vol. 52, pp. 1713–1730, Dec. 2015.
[30] D. Douglass, W. Chisholm, G. Davidson, I. Grant, K. Lindsey, M. Lancaster, D. Lawry, T. McCarthy, C. Nascimento, M. Pasha, J. Reding, T. Seppa, J. Toth, and P. Waltz, "Real-time overhead transmission-line monitoring for dynamic rating," *IEEE Trans. Power Del.*, vol. 31, no. 3, pp. 921–927, Jun. 2016.
[31] C. Mensah-Bonsu, U. F. Krekeler, G. T. Heydt, Y. Hoverson, J. Schilleci, and B. L. Agrawal, "Application of the global positioning system to the measurement of overhead power transmission conductor sag," *IEEE Trans. Power Del.*, vol. 17, no. 1, pp. 273–278, Jan. 2002.
[32] R. G. Olsen and K. S. Edwards, "A new method for real-time monitoring of high-voltage transmission-line conductor sag," *IEEE Trans. Power Del.*, vol. 17, no. 4, pp. 1142–1152, Oct. 2002.
[33] T. O. Seppa, "Accurate ampacity determination: Temperature-sag model for operational real time ratings," *IEEE Trans. Power Del.*, vol. 10, no. 3, pp. 1460–1470, Jul. 1995.
[34] S. M. Mahajan and U. M. Singareddy, "A real-time conductor sag measurement system using a differential GPS," *IEEE Trans. Power Del.*, vol. 27, no. 2, pp. 475–480, Apr. 2012.
[35] B. Fateh, M. Govindarasu, and V. Ajjarapu, "Wireless network design for transmission line monitoring in smart grid," *IEEE Trans. Smart Grid*, vol. 4, no. 2, pp. 1076–1086, Jun. 2013.
[36] W. Fatnassi and Z. Rezki, "Reliability enhancement of smart metering system using millimeter wave technology," *IEEE Trans. Commun.*, vol. 66, no. 10, pp. 4877–4892, Oct. 2018.
[37] M. Xiao, S. Mumtaz, Y. Huang, L. Dai, Y. Li, M. Matthaiou, G. K. Karagiannidis, E. Björnson, K. Yang, C.-L. I, and A. Ghosh, "Millimeter wave communications for future mobile networks," *IEEE J. Sel. Areas Commun.*, vol. 35, no. 9, pp. 1909–1935, Sep. 2017.
[38] A. U. Mahin and M. F. Hossain, "Millimeter wave based sag measurement technique for overhead transmission lines in smart-grid," in *Proc. Int. Conf. Energy Power Eng. (ICEPE)*, Dhaka, Bangladesh, Mar. 2019, pp. 1–5.
[39] A. U. Mahin, S. N. Islam, and M. F. Hossain, "Millimeter wave based sag measurement using parabolic approximation for smart grid overhead transmission line monitoring," in *Proc. IEEE Int. Conf. Commun., Control, Comput. Technol. Smart Grids (SmartGridComm)*, Beijing, China, Oct. 2019, pp. 1–5.
[40] T. S. Rappaport, Y. Xing, G. R. MacCartney, A. F. Molisch, E. Mellios, and J. Zhang, "Overview of millimeter wave communications for fifth-generation (5G) wireless networks-with a focus on propagation models," *IEEE Trans. Antennas Propag.*, vol. 65, no. 12, pp. 6219–6230, Dec. 2017.
[41] A. Badawy, T. Khattab, D. Trinchero, T. M. Elfouly, and A. Mohamed, "A simple cross correlation switched beam system (XSBS) for angle of arrival estimation," *IEEE Access*, vol. 5, pp. 3340–3352, 2017.
[42] B.-H. Son, K.-J. Kim, Y. Li, and Y.-W. Choi, "Active-margin transmission power control for wireless sensor networks," *Int. J. Distrib. Sensor Netw.*, vol. 10, no. 5, pp. 1–7, May 2014.
[43] O. Rioul and J. Magossi, "On Shannon's formula and Hartley's rule: Beyond the mathematical coincidence," *Entropy*, vol. 16, no. 9, pp. 4892–4910, Sep. 2014.
[44] S. S. Komaragiri and S. M. Mahajan, "A sag monitoring device based on a cluster of code based GPS receivers," in *Proc. IEEE Power Energy Soc. Gen. Meeting*, Calgary, Canada, Jul. 2009, pp. 1–7.
[45] S. Kamboj and R. Dahiya, "Designing and implementation of overhead conductor altitude measurement system using GPS for sag monitoring," in *Intelligent Computing Techniques for Smart Energy Systems*, vol. 607. 2020, pp. 183–194.
[46] A. H. Khawaja and Q. Huang, "Estimating sag and wind-induced motion of overhead power lines with current and magnetic-flux density measurements," *IEEE Trans. Instrum. Meas.*, vol. 66, no. 5, pp. 897–909, May 2017.
[47] X. Sun, K. S. Lui, K. K. Y. Wong, W. K. Lee, Y. Hou, Q. Huang, and P. W. T. Pong, "Novel application of magnetoresistive sensors for high-voltage transmission-line monitoring," *IEEE Trans. Magn.*, vol. 47, no. 10, pp. 2608–2611, Oct. 2011.
[48] A. Pavlinic and V. Komen, "Direct monitoring methods of overhead line conductor temperature," *Eng. Rev.*, vol. 37, no. 2, pp. 134–146, May 2017.
[49] E. Golinelli, S. Musazzi, U. Perini, and F. Barberis, "Conductors sag monitoring by means of a laser based scanning measuring system: Experimental results," in *Proc. IEEE Sensors Appl. Symp. Proc.*, Brescia, Italy, Feb. 2012, pp. 1–4.
[50] E. Golinelli, U. Perini, and G. Ogliari, "A new IR laser scanning system for power lines sag measurements," in *Proc. 18th Italian Nat. Conf. Photonic Technol. (Fotonica)*, Rome, Italy, 2016, pp. 1–4.

AYMAN UDDIN MAHIN received the B.Sc. degree in electrical and electronic engineering (EEE) from the Ahsanullah University of Science and Technology (AUST), Dhaka, Bangladesh, in 2016, and the M.Sc. degree in EEE from the Bangladesh University of Engineering and Technology (BUET), Dhaka, in 2019. He is currently working as a Lecturer with the Department of EEE, AUST. His research interests include smart grid communications, wireless sensor networks, the IoT, power systems, and demand side management.

MD. FARHAD HOSSAIN (Member, IEEE) received the B.Sc. and M.Sc. degrees in electrical and electronic engineering (EEE) from the Bangladesh University of Engineering and Technology (BUET), Dhaka, Bangladesh, in 2003 and 2005, respectively, and the Ph.D. degree from the School of Electrical and Information Engineering, The University of Sydney, Australia, in 2014. He is currently a Professor with BUET. He is also an Electrical and Electronic Engineering Consultant. He has published over 70 refereed articles in highly prestigious journals and conference proceedings in the field of wireless communications. His research interests include mobile cellular networks, the IoT and M2M communications, underwater communications, smart grid communications, wireless sensor networks, and satellite communications. He has been serving as a TPC member and a reviewer in many reputed international journals and conferences. He was a recipient of Best Paper Award in three different international conferences and the Student Travel Grant in IEEE Global Communications Conference (GLOBECOM), Anaheim, CA, USA, in 2012. He also received two awards—TransGrid Prize and SingTel Optus Prize in the category of Best Research Project in the Research Conversazione held in The University of Sydney, in 2012 and 2010, respectively.

SHAMA NAZ ISLAM received the bachelor's degree in electrical engineering from the Bangladesh University of Engineering and Technology, in 2009, and the Ph.D. degree from Australian National University, in 2015. She is currently a Senior Lecturer of electrical engineering with Deakin University. Her research interests are in smart grid communication, the IoT for smart energy applications, energy management, and smart grid security.

KUMUDU S. MUNASINGHE (Member, IEEE) received the Ph.D. degree in telecommunications engineering from The University of Sydney, Sydney, NSW, Australia, in 2008. He is currently an Associate Professor of network engineering and the Leader with the IoT Research Group, Human Centred Research Centre, Faculty of Science and Technology, School of IT and Systems, University of Canberra, Canberra, ACT, Australia. He also acts as an editorial board member and a reviewer for several prestigious international journals. His research interests include next-generation mobile networks, biologically and ecologically inspired networks, cloud networking, green communication systems, and smart grid communications. Dr. Munasinghe has been successful in securing several prestigious research grants and awards, such as ARC APD Fellowship, in 2010, ARC DP Grant, in 2010, USYD ECRS Grant, in 2012, USYD Bridging Support Seed Grant, in 2013, and Industrial Grants. He was a recipient of many research awards, including an IEEE Paper Award at the 50th Anniversary Global Communications Conference, Washington, DC, USA, in 2007. He has undertaken TPC Chairing responsibilities in a number of IEEE's flagship conferences.

ABBAS JAMALIPOUR (Fellow, IEEE) received the Ph.D. degree in electrical engineering from Nagoya University, Japan. He is currently a Professor of ubiquitous mobile networking with The University of Sydney, Australia. He has authored nine technical books, 11 book chapters, over 450 technical articles, and five patents, all in the area of wireless communications. Dr. Jamalipour is a Fellow of the Institute of Electrical, Information, and Communication Engineers (IEICE) and the Institution of Engineers, Australia, an ACM Professional Member, and an IEEE Distinguished Lecturer. He is an elected member of the Board of Governors, an Executive Vice-President, the Chair of Fellow Evaluation Committee, and the Editor-in-Chief of the Mobile World, IEEE Vehicular Technology Society. He has been a General Chair or Technical Program Chair of a number of conferences, including IEEE ICC, GLOBECOM, WCNC, and PIMRC. He was a recipient of a number of prestigious awards, such as the 2016 IEEE ComSoc Distinguished Technical Achievement Award in Communications Switching and Routing, the 2010 IEEE ComSoc Harold Sobol Award, the 2006 IEEE ComSoc Best Tutorial Paper Award, and 15 Best Paper Awards. He was the Editor-in-Chief of the IEEE Wireless Communications, the Vice President-Conference, and a member of Board of Governors of the IEEE Communications Society. He has been an editor of several journals.